Chapter 1

Solutions to Exercises

Chapter 2

Solutions to Exercises

EXERCISE 2.1. 1. Let $r(t) = \sqrt{r_0^2 + (vt)^2 + 2r_0 vt\cos(\phi)}$. Then,

$$E_r(f, t, r(t), \theta, \psi)) = \frac{\Re[\alpha(\theta, \psi, f)\exp\{j2\pi f(1 - r(t)/c)\}]}{r(t)}.$$

Moreover, if we assume that $r_0 \gg vt$, then we get that $r(t) \approx r_0 + vt\cos(\phi)$. Thus, the doppler shift is $fv\cos(\phi)/c$.

2. Let (x, y, z) be the position of the mobile in Cartesian coordinates, and (r, ψ, θ) the position in polar coordinates. Then

$$\begin{aligned}
(x, y, z) &= (r\sin\theta\cos\psi, r\sin\theta\sin\psi, r\cos\theta) \\
(r, \psi, \theta) &= \left(\sqrt{x^2 + y^2 + z^2}, \arctan(y/x), \arccos(z/\sqrt{x^2 + y^2 + z^2})\right) \\
\dot{\psi} &= \frac{x\dot{y} - \dot{x}y}{x^2 + y^2} \\
\dot{\theta} &= -\frac{\dot{z}r - z\dot{r}}{r^2\sqrt{1 - (z/r)^2}}
\end{aligned}$$

We see that $\dot{\psi}$ is small for large $x^2 + y^2$. Also $\dot{\theta}$ is small for $|z/r| < 1$ and r large. If $|r/z| = 1$ then $\theta = 0$ or $\theta = \pi$ and $v <= r|\dot{\theta}|$ so v/r large assures that $\dot{\theta}$ is small. If r is not very large then the variation of θ and ψ may not be negligible within the time scale of interest even for moderate speeds v. Here large depends on the time scale of interest.

EXERCISE 2.2.

$$\begin{aligned}
E_r(f, t) &= \frac{\alpha\cos\left[2\pi f\left(t - r(t)/c\right)\right]}{2d - r(t)} + \frac{2\alpha\left[d - r(t)\right]\cos\left[2\pi f\left(t - r(t)/c\right)\right]}{r(t)[2d - r(t)]} \\
&\quad - \frac{\alpha\cos\left[2\pi f\left(t + (r(t) - 2d)/c\right)\right]}{2d - r(t)}
\end{aligned}$$

$$= \frac{2\alpha \sin\left[2\pi f\left(t - d/c\right)\right]\sin\left[2\pi f\left(r(t) - d\right)/c\right]}{2d - r(t)} + \frac{2\alpha\left[d - r(t)\right]\cos\left[2\pi f\left(t - r(t)/c\right)\right]}{r(t)[2d - r(t)]} \tag{2.1}$$

where we applied the identity

$$\cos x - \cos y = 2\sin\left(\frac{x+y}{2}\right)\sin\left(\frac{y-x}{2}\right)$$

We observe that the first term of (2.1) is similar in form to equation (2.13) in the notes. The second term of (2.1) goes to 0 as $r(t) \to d$ and is due to the difference in propagation losses in the 2 paths.

Exercise 2.3. If the wall is on the other side, both components arrive at the mobile from the left and experience the same Doppler shift.

$$E_r(f,t) = \frac{\Re[\alpha \exp\{j2\pi[f(1-v/c)t - fr_0/c]\}]}{r_0 + vt} - \frac{\Re[\alpha \exp\{j2\pi[f(1-v/c)t - f(r_0+2d)/c]\}]}{r_0 + 2d + vt}$$

We have the interaction of 2 sinusoidal waves of the same frequency and different amplitude.

Over time, we observe the composition of these 2 waves into a single sinusoidal signal of frequency $f(1-v/c)$ and constant amplitude that depends on the attenuations $(r_0 + vt)$ and $(r_0 + 2d + vt)$ and also on the phase difference $f2d/c$.

Over frequency, we observe that when $f2d/c$ is an integer both waves interfere destructively resulting in a small received signal. When $f2d/c = (2k+1)/2, k \in Z$ these waves interfere constructively resulting in a larger received signal. So when f is varied by $c/4d$ the amplitude of the received signal varies from a minimum to a maximum.

The variation over frequency is similar in nature to that of section 2.1.3, but since the delay spread is different the coherence bandwidth is also different.

However there is no variation over time because the Doppler spread is zero.

Exercise 2.4. 1. i) With the given information we can compute the Doppler spread:

$$D_s = |f_1 - f_2| = \frac{fv}{c}|\cos\theta_1 - \cos\theta_2|$$

from which we can compute the coherence time

$$T_c = \frac{1}{4D_s} = \frac{c}{4fv|\cos\theta_1 - \cos\theta_2|}$$

ii) There is not enough information to compute the coherence bandwidth, as it depends on the delay spread which is not given. We would need to know the difference in path length to compute the delay spread T_d and use it to compute W_c.

2. From part 1 we see that a larger angular range results in larger delay spread and smaller coherence time. Then, in the richly scattered environment the channel would show a smaller coherence time than in the environment where the reflectors are clustered in a small angular range.

EXERCISE 2.5. 1.

$$\begin{aligned}
r_1 &= \sqrt{r^2+(h_s-h_r)^2} = r\sqrt{1+(h_s-h_r)^2/r^2} \approx r(1+\frac{(h_s-h_r)^2}{2r^2}) \\
r_2 &= \sqrt{r^2+(h_s+h_r)^2} = r\sqrt{1+(h_s+h_r)^2/r^2} \approx r(1+\frac{(h_s+h_r)^2}{2r^2}) \\
r_2-r_1 &\approx \frac{(h_s+h_r)^2-(h_s-h_r)^2}{2r} = \frac{h_s^2+h_r^2+2h_sh_r-h_s^2-h_r^2+2h_sh_r}{2r} \\
&= \frac{2h_sh_r}{r}
\end{aligned}$$

Therefore $b = 2h_sh_r$.

2.

$$\begin{aligned}
E_r(f,t) &\approx \frac{Re[\alpha[\exp\{j2\pi(ft-fr_1/c)] - \exp\{j2\pi(ft-fr_2/c)]]}{r_1} \\
&= \frac{Re[\alpha[\exp\{j2\pi(ft-fr_1/c)][1-\exp(j2\pi f(r_1-r_2)/c)]}{r_1} \\
&\approx \frac{Re[\alpha[\exp\{j2\pi(ft-fr_1/c)][1-\exp(j2\pi f/c*b/r)]}{r_1} \\
&\approx \frac{Re[\alpha[\exp\{j2\pi(ft-fr_1/c)][1-(1-j2\pi f/c*b/r)]}{r_1} \\
&= \frac{2\pi f|\alpha|b}{cr^2}\Re[j\exp(j\angle\alpha)\exp[j2\pi(ft-fr_1/c)]] \\
&= -\frac{2\pi f|\alpha|b}{cr^2}\sin[2\pi(ft-fr_1/c)+\angle\alpha]]
\end{aligned}$$

Therefore $\beta = 2\pi f|\alpha|b/c$.

3.

$$\frac{1}{r_2} = \frac{1}{r_1+(r_2-r_1)} = \frac{1}{r_1[1+(r_2-r_1)/r_1]} \approx \frac{1}{r_1}\left(1-\frac{r_2-r_1}{r_1}\right) \approx \frac{1}{r_1}\left(1-\frac{b}{r_1^2}\right)$$

Therefore if we don't make the approximation of b) we get another term in the expansion that decays as r^{-3}. This term is negligible for large enough r as compared to β/r^2.

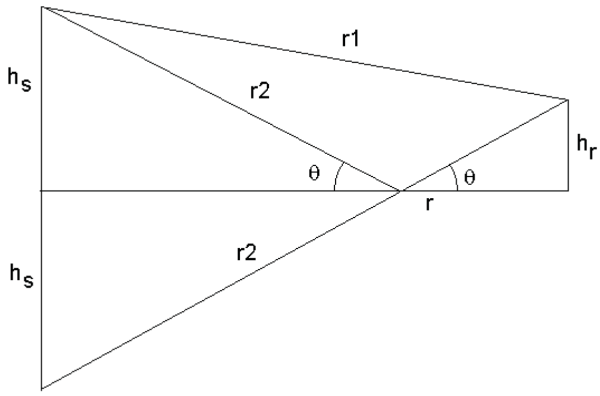

EXERCISE 2.6. 1. Let f_2 be the probability density of the distance from the origin at which the photon is absorbed by exactly the 2nd obstacle that it hits. Let x be the location of the first obstacle, then

$$\begin{aligned} f_2(r) &= \mathbb{P}\{\text{photon absorbed by 2nd obstacle at } r\} \\ &= \int_x \mathbb{P}\{\text{absorbed by 2nd obstacle at } r \mid \text{not absorbed by 1st obstacle at } x\} \\ &\qquad \times\ \mathbb{P}\{\text{not absorbed by 1st obstacle at } x\} \quad dx \end{aligned}$$

Since the obstacle are distributed according to poisson process which has memoryless distances between consecutive points, the first term inside the integral is $f_1(r-x)$. The second term is the probability that the first obstacle is at x and the photon is not absorbed by it. Thus, it is given by $(1-\gamma)q(x)$. Thus,

$$f_2(r) = \int_{x=-\infty}^{\infty} (1-\gamma)q(x)f_1(r-x)dx$$

2. Similarly, we observe that $f_{k+1}(r)$ is given by

$$\begin{aligned} f_{k+1}(r) &= \int_x \mathbb{P}\{\text{absorbed by } (k+1)\text{th obst at } r \mid \text{not absorbed by 1st obst at } x\} \\ &\qquad \times\ \mathbb{P}\{\text{not absorbed by 1st obstacle at } x\} \quad dx \\ &= \int_{x=-\infty}^{\infty} (1-\gamma)q(x)f_k(r-x)dx \end{aligned} \tag{2.2}$$

3. Summing up (2.2) for $k = 1$ to ∞, we get:

$$\sum_{k=2}^{\infty} f_k(r) = \int_{x=-\infty}^{\infty} (1-\gamma)q(x) \left(\sum_{k=1}^{\infty} f_k(r-x) \right) dx$$

Thus,

$$f(r) - f_1(r) = \int_{x=-\infty}^{\infty} (1-\gamma)q(x)f(r-x)dx,$$

or equivalently,

$$f(r) = \gamma q(r) + \int_{x=-\infty}^{\infty} (1-\gamma)q(x)f(r-x)dx \tag{2.3}$$

4. Using (2.3), we get that

$$F(\omega) = (1-\gamma)Q(\omega) + F(\omega)Q(\omega), \tag{2.4}$$

where F and Q denote the Fourier transform of f and q respectively. Since the $q(x)$ is known explicitly, its Fourier transform can be directly calculated and it turns out to be:

$$Q(\omega) = \frac{\eta^2}{\eta^2 + \omega^2}.$$

Substituting thin in (2.4), we get

$$F(\omega) = \frac{\gamma\eta^2}{\gamma\eta^2 + \omega^2}.$$

Thus, F is of the same form as Q, except for a different parameter η. Thus,

$$f(r) = \frac{\sqrt{\gamma}\eta}{2} e^{-\sqrt{\gamma}\eta|r|}$$

5. Without any loss of generality we can assume that r is positive, then power density at r is given by

$$\begin{aligned} \int_{x=r}^{\infty} f(x)dx &= \int_{x=r}^{\infty} \frac{\sqrt{\gamma}\eta}{2} e^{-\sqrt{\gamma}\eta x} dx \\ &= \frac{1}{2} e^{-\sqrt{\gamma}\eta r}. \end{aligned}$$

A similar calculation for a negative r gives power density at distance r to be

$$\frac{e^{-\sqrt{\gamma}\eta|r|}}{2}.$$

Exercise 2.7.

EXERCISE 2.8. The block diagram for the (unmodified) system is:

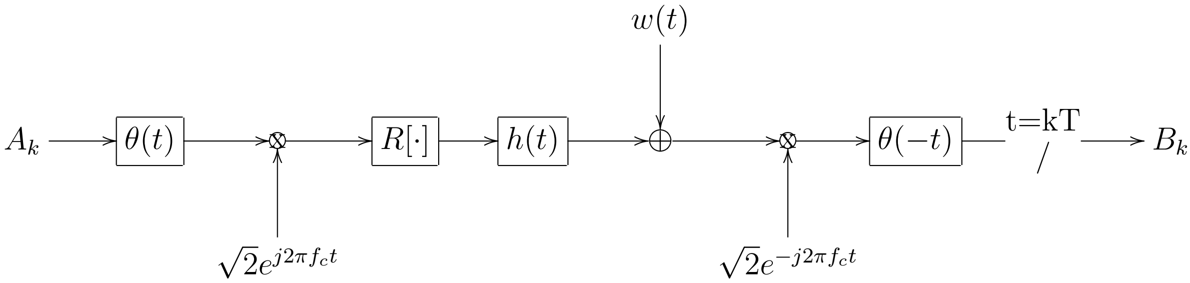

1. Which filter should one redesign?

One should redesign the filter at the transmitter. Modifying the filter at the receiver may cause $\{\theta(t-kT)\}_k$ no longer to be an orthonormal set, resulting in noise on the samples not to be i.i.d. By leaving $\{\theta(t-kT)\}_k$ at the receiver as an orthonormal set, we are assured the the noise on the samples is i.i.d.

Let the modified filter be g(t). The block diagram for the modified system is:

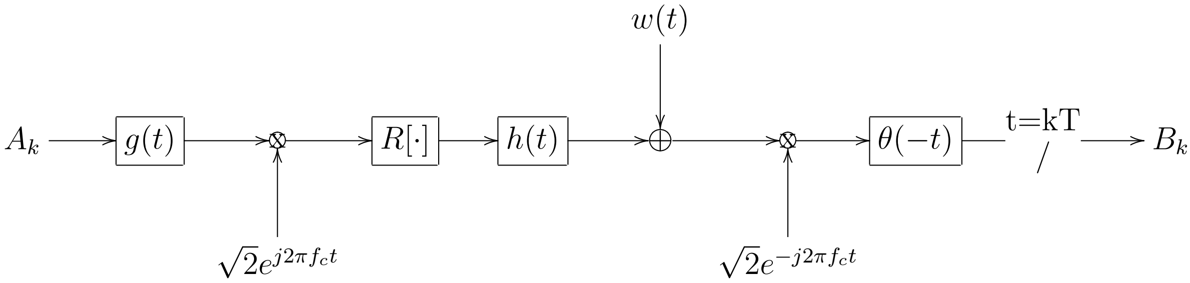

(Solution to Part 3: Figure of the various filters at passband).

We want to find g(t) such that there is no ISI between samples. Before we continue to find g(t), we depict the desired simplified block diagram for the system with no ISI:

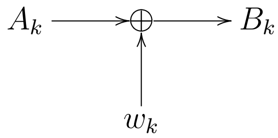

For ease of manipulation, we transform the passband representation of the system to a baseband representation

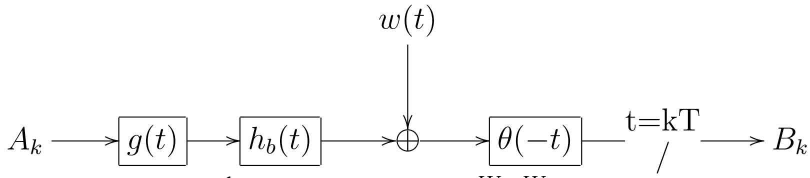

where $H_b(f) = \begin{cases} H(f+f_c) & \in [-\frac{W}{2}, \frac{W}{2}] \\ 0 & \text{otherwise} \end{cases}$

$H(f)$ is assumed bandlimited between $[f_c - \frac{W}{2}, f_c + \frac{W}{2}]$

We let $g(t) = \sum_k g_k \theta(t-kT)$, and redraw the block diagram:

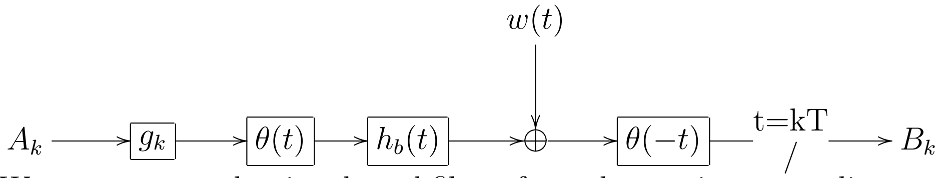

We now convert the signals and filters from the continuous to discrete time domain:

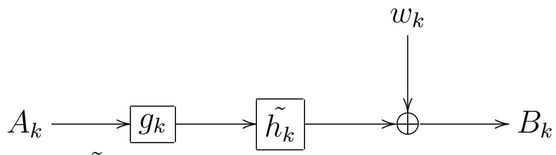

where $\tilde{h}_k = \theta * h_b * \theta_-|_{t=kT}$.

We justify interchanging the order of w(t) and $\theta(-t)$, since we know the noise on the samples is i.i.d.

$G(z) = \tilde{H}^{-1}(z)$ gives the desired result.

In summary, $g(t) = \sum_k g_k \theta(t - kT)$ where g_k is given by $G(z) = \tilde{H}^{-1}(z)$, and $\tilde{H}(z)$ is given by the Z-Transform of $\tilde{h}_k = \theta * h_b * \theta_-|_{t=kT}$

Exercise 2.9. Part 1)

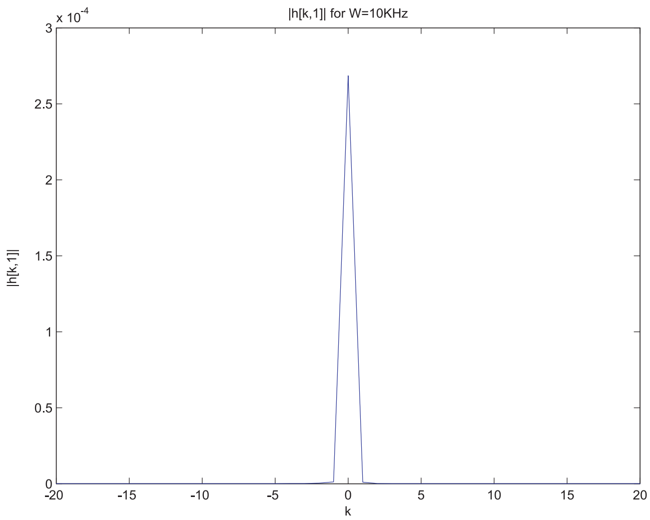

Figure 2.1: Magnitude of taps, W = 10kHz, time = 1 sec. Two paths are completely lumped together

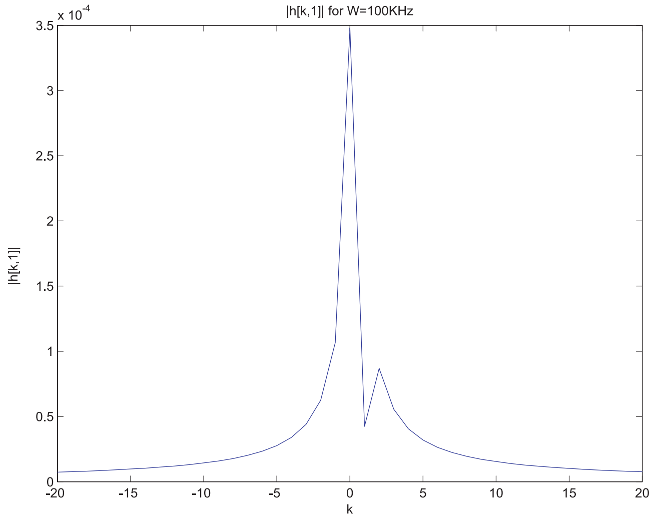

Figure 2.2: Magnitude of taps, W = 100kHz, time = 1 sec. Two paths are starting to become resolved.

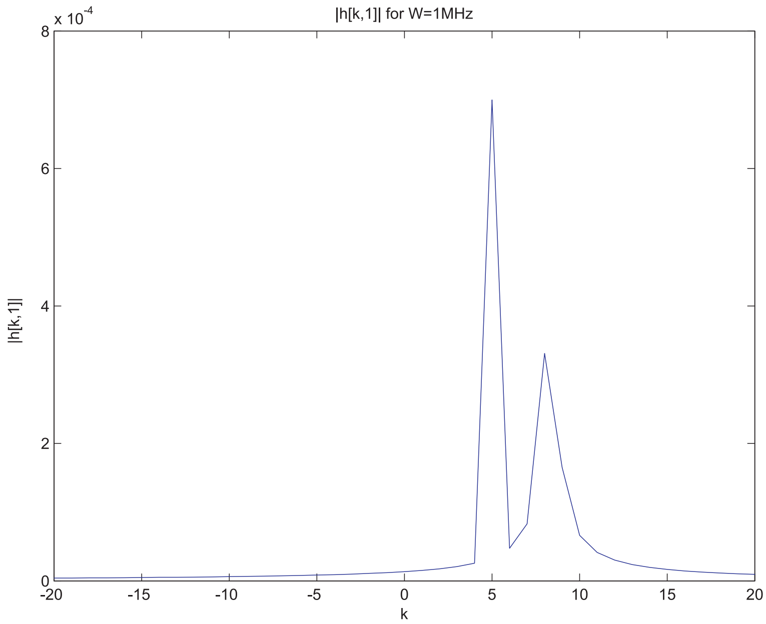

Figure 2.3: Magnitude of taps, W = 1MHz, time = 1 sec. Two paths are more resolved.

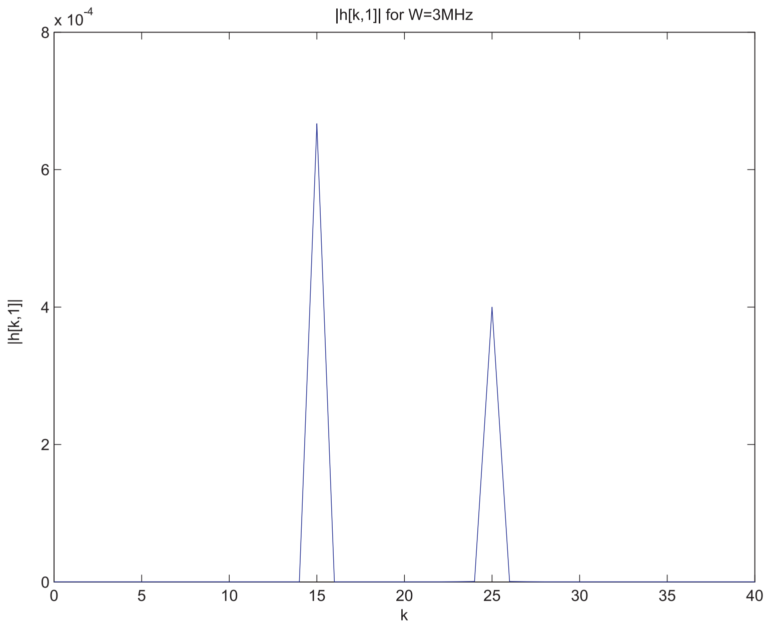

Figure 2.4: Magnitude of taps, W = 3MHz, time = 1 sec. Two paths are clearly resolved.

Part 2) We see that the time variations have the same frequency in both cases (flat fading in Figure 2.5 and frequency selective fading in Figure 2.7), but are much more pronounced in the case of flat fading. This is because in frequency selective fading (large W) each of the signal paths corresponds to a different tap, so they don't interfere significantly and the taps have small fluctuations. On the other hand in the case of flat fading, we sample the channel impulse response with low resolution and all the signal paths are lumped into the same tap. They interfere constructively and destructively generating large fluctuations in the tap values. If the model included more signal paths, then the number of paths contributing significantly to each tap would vary as a function of the bandwidth W, so the frequency of the tap variations would depend on the bandwidth, smaller bandwidth corresponding to larger Doppler spread and faster fluctuations (smaller T_c). Finally we could analyze this effect in the frequency domain. In frequency selective fading, the channel frequency response varies within the bandwidth of interest. There is an averaging effect and the resulting signal is never faded too much. This is an example of diversity over frequency.

Exercise 2.10. Consider the environment in Figure 2.9.

The shorter paths (dotted lines) contribute to the first tap and the longer paths (dashed) contribute to the second tap. Then the delay spread for the first tap is given by:

$$\frac{fv}{c}|\cos\phi_1 - \cos\phi_2|,$$

and the delay spread for the second tap is given by:

$$\frac{fv}{c}|\cos\theta_1 - \cos\theta_2|.$$

By appropriately choosing $\theta_1, \theta_2, \phi_1$ and ϕ_2, we can construct examples where the doppler spreads for both the taps are same or different.

Exercise 2.11. Let $H(f) = 1$ for $|f| < W/2$ and 0 otherwise. Then if $h(t) \leftrightarrow H(f)$ it follows that $h(t) = W\text{sinc}(Wt)$. Then we can write:

$$\begin{aligned}
\Re\{w[m]\} &= \left\{[w(t)\sqrt{2}\cos(2\pi f_c t)] * h(t)\ |_{t=m/W}\right\} \\
&= \left[\int_{-\infty}^{\infty} w(\tau)\sqrt{2}W\cos(2\pi f_c\tau)\text{sinc}(W(t-\tau))d\tau\right]_{t=m/W} \\
&= \int_{-\infty}^{\infty} w(\tau)\sqrt{2}W\cos(2\pi f_c\tau)\text{sinc}(m - W\tau)d\tau \\
&= \int_{-\infty}^{\infty} w(\tau)\psi_{m,1}(\tau)d\tau
\end{aligned}$$

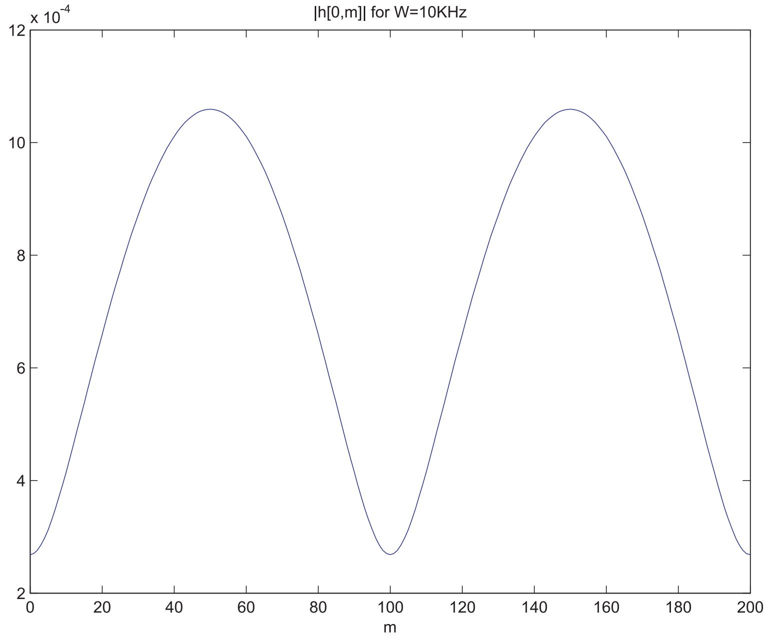

Figure 2.5: Flat fading: time variation of magnitude of 1 tap. (x-axis is the time index m).

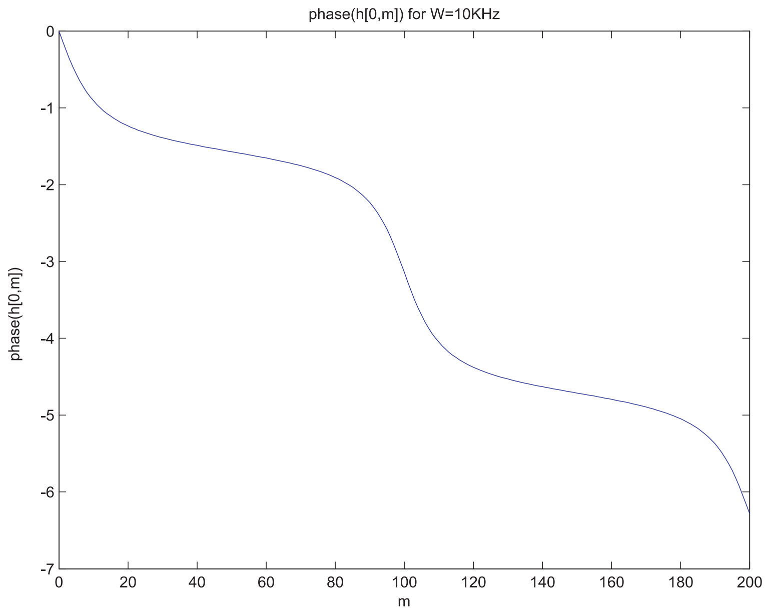

Figure 2.6: Flat fading: time variation of phase of 1 tap. (x-axis is the time index m).

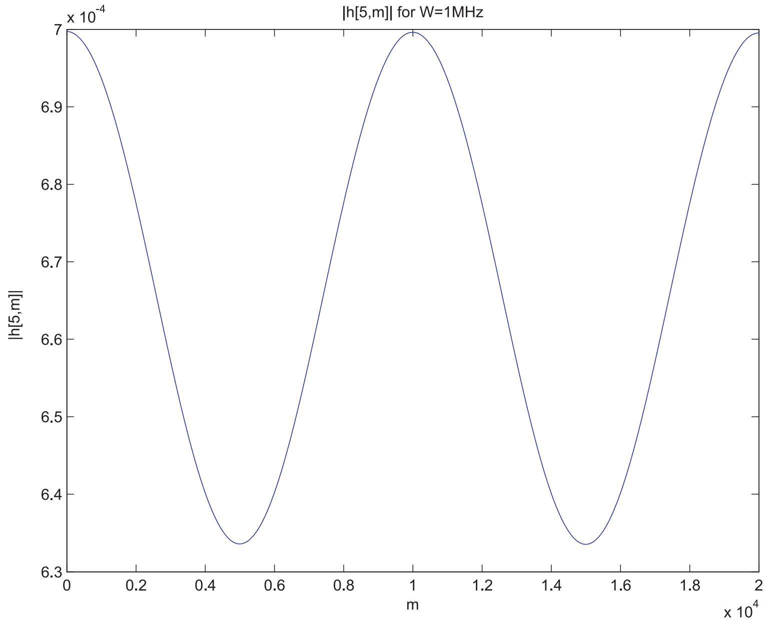

Figure 2.7: Frequency selective fading: time variation of magnitude of 1 tap. Note: scale of y-axis is much finer here than in the flat fading case. (x-axis displays time with units of seconds. x-axis label of time index 'm' is a typo. Should be 'time.')

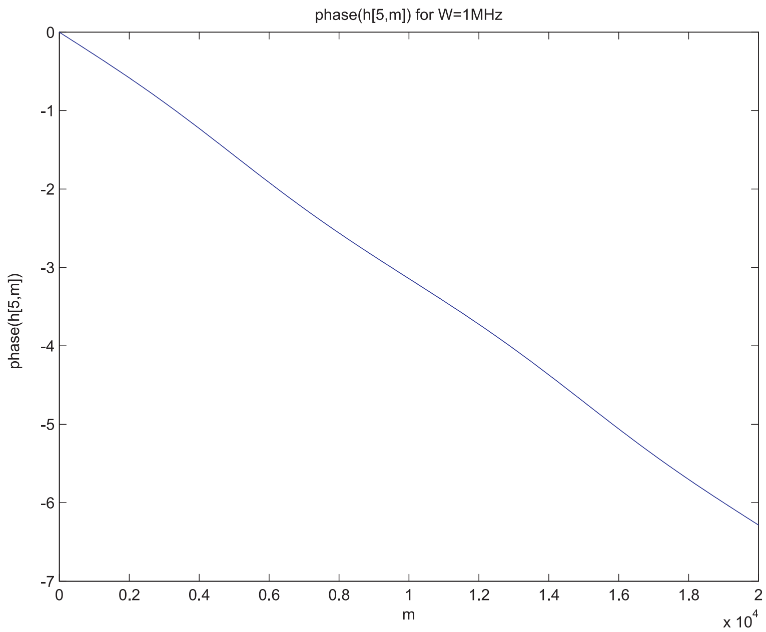

Figure 2.8: Frequency selective fading: time variation of phase of 1 tap. (x-axis displays time with units of seconds. x-axis label of time index 'm' is a typo. Should be 'time.')

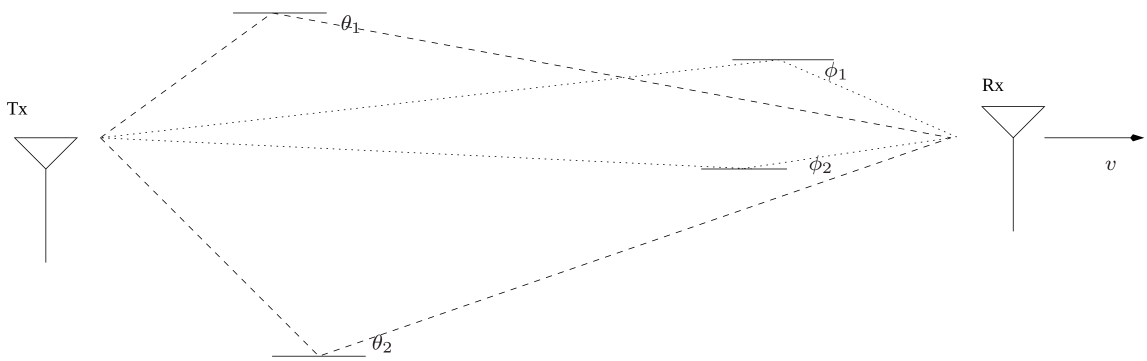

Figure 2.9: Location of reflectors, transmitter and receiver

where $\psi_{m,1}(\tau) = \sqrt{2}W cos(2\pi f_c \tau)\text{sinc}(m - W\tau)$.

Similarly,

$$\begin{aligned}
\Im\{w[m]\} &= -\left\{[w(t)\sqrt{2}\sin(2\pi f_c t)] * h(t) \mid_{t=m/W}\right\} \\
&= -\left[\int_{-\infty}^{\infty} w(\tau)\sqrt{2}W \sin(2\pi f_c \tau)\text{sinc}(W(t-\tau))d\tau\right]_{t=m/W} \\
&= -\int_{-\infty}^{\infty} w(\tau)\sqrt{2}W \sin(2\pi f_c \tau)\text{sinc}(m - W\tau)d\tau \\
&= \int_{-\infty}^{\infty} w(\tau)\psi_{m,2}(\tau)d\tau
\end{aligned}$$

where $\psi_{m,2}(\tau) = -\sqrt{2}W sin(2\pi f_c \tau)\text{sinc}(m - W\tau)$.

EXERCISE 2.12. 1) Let $\theta_n(t)$ denote $\theta(t - nT)$.

Show that if the waveforms $\{\theta_n(t)\}_n$ form an orthogonal set, then the waveforms $\{\psi_{n,1}, \psi_{n,2}\}_n$ also form an orthogonal set, provided $\theta(t)$ is band-limited to $[-f_c, f_c]$. $\psi_{n,1}, \psi_{n,2}$ are defined as

$$\begin{aligned}
\psi_{n,1}(t) &= \theta_n(t)\cos 2\pi f_c t \\
\psi_{n,2}(t) &= \theta_n(t)\sin 2\pi f_c t
\end{aligned} \tag{2.5}$$

By definition $\{\theta_n(t)\}_n$ forms an orthogonal set

$$\begin{aligned}
&\iff \quad \int_{-\infty}^{\infty} \theta_n^*(t)\theta_m(t)dt = a\,\delta[m-n] \quad \text{for some } a \in \mathbb{R} \\
&\iff \quad \int_{-\infty}^{\infty} \Theta_n^*(f)\Theta_m(f)df = a\,\delta[m-n] \quad \text{for some } a \in \mathbb{R}, \text{ by Parseval's Theorem(2.6)}
\end{aligned}$$

where $\Theta_n(f)$ is the Fourier Transform of $\theta_n(t)$.

We would like to show

1) $< \psi_{n,1}(t), \psi_{m,1}(t) > \;\propto\; \delta[m-n] \quad \forall\, m,n \in \mathbb{Z}$
waveforms modulated by $\cos 2\pi f_c t$ remain orthogonal to each other

2) $< \psi_{n,2}(t), \psi_{m,2}(t) > \;\propto\; \delta[m-n] \quad \forall\, m,n \in \mathbb{Z}$
waveforms modulated by $\sin 2\pi f_c t$ remain orthogonal to each other

3) $< \psi_{n,1}(t), \psi_{m,2}(t) > \;=\; 0 \quad \forall\, m,n \in \mathbb{Z}$
waveforms modulated by $\cos 2\pi f_c t$ are orthog. to waveforms modulated by $\sin 2\pi f_c t$.

We will show these three cases individually:
Case 1)

$$
\begin{aligned}
< \psi_{n,1}(t), \psi_{m,1}(t) > &= \int_{-\infty}^{\infty} \psi_{n,1}^*(t)\psi_{m,1}(t)dt \\
&= \int_{-\infty}^{\infty} \Psi_{n,1}^*(f)\Psi_{m,1}(f)df \text{ by Parseval's} \qquad (2.7)
\end{aligned}
$$

where

$$
\begin{aligned}
\Psi_{n,1}(f) &= \int_{-\infty}^{\infty} \psi_{n,1}(t)e^{-j2\pi ft}dt \\
&= \int_{-\infty}^{\infty} \theta_n(t)\cos(2\pi f_c t)e^{-j2\pi ft}dt, \qquad \text{from (2.5)} \\
&= \Theta_n(f) * (\frac{1}{2}\delta(f-f_c) + \frac{1}{2}\delta(f+f_c)) \\
&= \frac{1}{2}(\Theta_n(f-f_c) + \Theta_n(f+f_c))
\end{aligned}
$$

Substituting into (3)

$$
\begin{aligned}
&= \frac{1}{4}\int_{-\infty}^{\infty} [\Theta_n^*(f-f_c) + \Theta_n^*(f+f_c)][\Theta_m(f-f_c) + \Theta_m(f+f_c)]df \\
&= \frac{1}{4}\int_{-\infty}^{\infty} \Theta_n^*(f-f_c)\Theta_m(f-f_c) + \underbrace{\Theta_n^*(f-f_c)\Theta_m(f+f_c)}_{=0} + \\
&\quad + \underbrace{\Theta_n^*(f+f_c)\Theta_m(f-f_c)}_{=0} + \Theta_n^*(f+f_c)\Theta_m(f+f_c)df
\end{aligned}
$$

The second and third terms equal zero since $\theta(t)$ is bandlimited to $[-f_c, f_c]$ resulting in no overlap in the region of support of $\Theta(f+f_c)$ and $\Theta(f-f_c)$, as seen in Figure 2.10(b).

$$
= \frac{1}{4}\int_{-\infty}^{\infty} \Theta_n^*(f-f_c)\Theta_m(f-f_c) + \Theta_n^*(f+f_c)\Theta_m(f+f_c)df
$$

$$= \frac{1}{4}\int_{-\infty}^{\infty} \Theta_n^*(f)\Theta_m(f) + \Theta_n^*(f)\Theta_m(f)df$$

since integrals from $-\infty$ to ∞ are invariant to shifts of the integrand along the x-axis.

$$\begin{aligned}
&= \frac{1}{4}2\int_{-\infty}^{\infty} \Theta_n^*(f)\Theta_m(f)df \\
&= \frac{a}{2}\delta[m-n], \text{ by equation (2.6)} \qquad (2.8) \\
&\propto \delta[m-n]
\end{aligned}$$

Case 2)
$< \psi_{n,2}(t), \psi_{m,2}(t) >$

$$\begin{aligned}
&= \int_{-\infty}^{\infty} \psi_{n,2}^*(t)\psi_{m,2}(t)dt \\
&= \int_{-\infty}^{\infty} \Psi_{n,2}^*(f)\Psi_{m,2}(f)df \text{ by Parseval's} \\
&= \int_{-\infty}^{\infty} (\frac{1}{2j})^*[\Theta_n^*(f-f_c) - \Theta_n^*(f+f_c)](\frac{1}{2j})[\Theta_m(f-f_c) - \Theta_m(f+f_c)]df \\
&= \frac{1}{4}\int_{-\infty}^{\infty} \Theta_n^*(f-f_c)\Theta_m(f-f_c) - \underbrace{\Theta_n^*(f-f_c)\Theta_m(f+f_c)}_{=0} + \\
&\quad - \underbrace{\Theta_n^*(f+f_c)\Theta_m(f-f_c)}_{=0} + \Theta_n^*(f+f_c)\Theta_m(f+f_c)df \\
&= \frac{1}{4}\int_{-\infty}^{\infty} \Theta_n^*(f-f_c)\Theta_m(f-f_c) + \Theta_n^*(f+f_c)\Theta_m(f+f_c)df \\
&= \frac{1}{4}\int_{-\infty}^{\infty} \Theta_n^*(f)\Theta_m(f) + \Theta_n^*(f)\Theta_m(f)df \\
&= \frac{1}{4}2\int_{-\infty}^{\infty} \Theta_n^*(f)\Theta_m(f)df \\
&= \frac{a}{2}\delta[m-n], \text{ by equation (2.6)} \qquad (2.9) \\
&\propto \delta[m-n]
\end{aligned}$$

Case 3)
$< \psi_{n,1}(t), \psi_{m,2}(t) >$

$$\begin{aligned}
&= \int_{-\infty}^{\infty} \psi_{n,1}^*(t)\psi_{m,2}(t)dt \\
&= \int_{-\infty}^{\infty} \Psi_{n,1}^*(f)\Psi_{m,2}(f)df \text{ by Parseval's}
\end{aligned}$$

$$
\begin{aligned}
&= (\frac{1}{4j})\int_{-\infty}^{\infty}[\Theta_n^*(f-f_c)+\Theta_n^*(f+f_c)][\Theta_m(f-f_c)-\Theta_m(f+f_c)]df \\
&= (\frac{1}{4j})\int_{-\infty}^{\infty}\Theta_n^*(f-f_c)\Theta_m(f-f_c)-\underbrace{\Theta_n^*(f-f_c)\Theta_m(f+f_c)}_{=0}+ \\
&\quad +\underbrace{\Theta_n^*(f+f_c)\Theta_m(f-f_c)}_{=0}-\Theta_n^*(f+f_c)\Theta_m(f+f_c)df \\
&= (\frac{1}{4j})\int_{-\infty}^{\infty}\Theta_n^*(f-f_c)\Theta_m(f-f_c)-\Theta_n^*(f+f_c)\Theta_m(f+f_c)df \\
&= (\frac{1}{4j})\int_{-\infty}^{\infty}\Theta_n^*(f)\Theta_m(f)-\Theta_n^*(f)\Theta_m(f)df \\
&= 0 \quad \forall\, m,n\in\mathbb{Z}
\end{aligned}
$$

For $\psi(t)$ to be *orthonormal*, set $\frac{a}{2}=1$ in (2.8) and (2.9), which implies $a=2$. We should scale $\theta_n(t)$ by $\sqrt{2}$.

Part 2) $\tilde{\theta}(t)=4f_c\mathrm{sinc}(4f_ct)$ is an example $\theta(t)$ that is *not* band-limited to $[-f_c,f_c]$. See Figure 2.10(c). For this example, there will be an overlap in the region of support of $\tilde{\Theta}(f+f_c)$ and $\tilde{\Theta}(f-f_c)$. See Figure 2.10(d). The cross terms $\tilde{\Theta}_n^*(f-f_c)\tilde{\Theta}_m(f+f_c)$ and $\tilde{\Theta}_n^*(f+f_c)\tilde{\Theta}_m(f-f_c)$ will no longer $=0$ and $\{\psi_{n,1},\psi_{n,2}\}_n$ will no longer by orthogonal.

2 take away messages:
1) The orthogonality property of a set of waveforms is unchanged if the waveforms experience a frequency shift, or in other words are multiplied by $e^{j2\pi f_ct}$.
2) WGN projected onto $\{\psi_{n,1},\psi_{n,2}\}_n$ will yield i.i.d. gaussian noise samples.

EXERCISE 2.13. Let $\mathbf{F}[\cdot]$ denote the Fourier transform operator, $*$ denote convolution, $u(\cdot)$ the unit step function and

$$
H(f)=\begin{cases} 1/j & if \quad f>0 \\ 0 & if \quad f=0 \\ -1/j & if \quad f<0 \end{cases}
$$

with $h(t)\leftrightarrow H(f)$. Then we can write:

$$
\begin{aligned}
\Im[y_b(t)e^{j2\pi f_ct}] &= \frac{1}{2j}[y_b(t)e^{j2\pi f_ct}-(y_b(t)e^{j2\pi f_ct})^*]=\frac{1}{2j}\mathbf{F}^{-1}[Y_b(f-f_c)-Y_b^*(-f-f_c)] \\
&= \frac{\sqrt{2}}{2j}\mathbf{F}^{-1}[Y(f)u(f)-Y(f)u(-f)]=\frac{\sqrt{2}}{2}\mathbf{F}^{-1}[Y(f)H(f)]=\frac{\sqrt{2}}{2}y(t)*h(t) \\
&= \frac{\sqrt{2}}{2}\sum_i[a_i(t)x(t-\tau_i(t))]*h(t)
\end{aligned}
$$

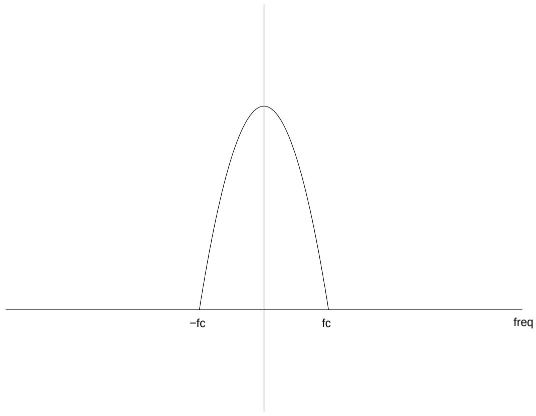

(a) Frequency range of $\Theta(f)$ band-limited from $-f_c, f_c$

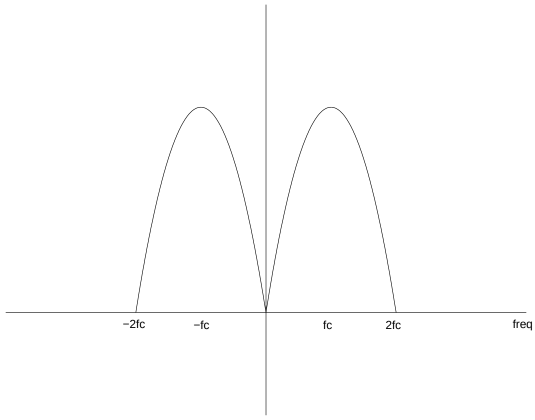

(b) Frequency range of $\Theta(f+fc)$ and $\Theta(f-fc)$. Notice no overlap in region of support.

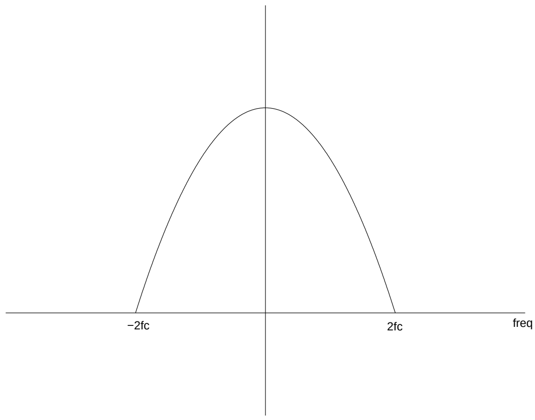

(c) Frequency range of $\tilde{\Theta}(f)$ *not* band-limited from $-f_c, f_c$

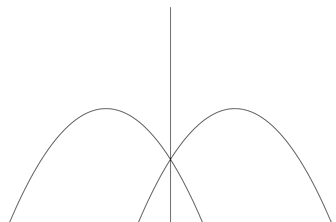

$$
\begin{aligned}
&= \frac{\sqrt{2}}{2}\sum_i \{a_i(t)\sqrt{2}\Re[x_b(t-\tau_i(t))e^{j2\pi f_c(t-\tau_i(t))}]\} * h(t) \\
&= \frac{1}{2}\sum_i \{a_i(t)[x_b(t-\tau_i(t))e^{j2\pi f_c(t-\tau_i(t))} + x_b^*(t-\tau_i(t))e^{-j2\pi f_c(t-\tau_i(t))}]\} * h(t) \\
&=_a \frac{1}{2j}\sum_i \{a_i(t)[x_b(t-\tau_i(t))e^{j2\pi f_c(t-\tau_i(t))} - x_b^*(t-\tau_i(t))e^{-j2\pi f_c(t-\tau_i(t))}]\} \\
&= \sum_i \{a_i(t)\Im[x_b(t-\tau_i(t))e^{j2\pi f_c(t-\tau_i(t))}]\} \\
&= \Im\left\{\left[\sum_i a_i(t)x_b(t-\tau_i(t))e^{-j2\pi f_c\tau_i(t)}\right]e^{j2\pi f_c t}\right\}
\end{aligned}
$$

The equality (a) follows because the first term between the braces is zero for negative frequencies and the second term is zero for positive frequencies.

Yes. Both equations together allow to equate the complex arguments of the $\Re$ and $\Im$ operators, thus allowing to obtain the baseband equivalent of the impulse response of the channel.

Exercise 2.14.

Exercise 2.15. Effects that make the tap gains vary with time:

- Doppler shifts and Doppler spread: $D = f_c\tau_i'(t)$, $T_c \sim 1/D = 1/(f_c\tau_i'(t))$ The coherence time is determined by the Doppler spread of the paths that contribute to a given tap. As W increases the paths are sampled at higher resolution and fewer paths contribute to each tap. Therefore the Doppler spread decreases for increasing W and its influence on the variation of the tap gains decreases.

- Variation of $\{a_i(t)\}_i$ with time. $a_i(t)$ changes slowly, with a time scale of variation much larger than the other effects discussed. However as W increases and it becomes comparable to f_c assuming that a single gain affects the corresponding path equally across all frequencies may not be a good approximation. The reflection coefficient of the scatterers may be frequency dependent and for very large bandwidths we need to change the model.

- Movement of paths from tap to tap. $\tau_i(t)$ changes with t and the corresponding path moves from one tap to another. As W increases fewer paths contribute to each tap and the tap gains change significantly when a path moves from tap to tap. A path moves from tap to tap when $\Delta\tau_i(t)W = 1$ or $\Delta\tau_i(t)/\Delta t \cdot W = 1/\Delta t$. So this effect takes place in a time scale of $\Delta t \sim 1/(W\tau_i'(t))$. As W increases this effect starts taking place in a small time scale and it becomes the dominant cause of time variation in the channel tap gains.

The third effect dominates when $\Delta t < T_c$ or equivalently when $W > f_c$.

EXERCISE 2.16.

$$h_\ell[m] = \sum_{i=1}^{N} a_i(m/W) e^{-j2\pi f_c \tau_i(m/W)} \text{sinc}(\ell - \tau_i(m/W)W)$$

Let $\bar{\tau} = \frac{1}{N}\sum_{i=1}^{N} \tau_i(0)$ and $\Delta\tau_i(m/W) = \tau_i(m/W) - \bar{\tau}$. Then,

$$h_\ell[m] = e^{-j2\pi f_c \bar{\tau}} \sum_{i=1}^{N} a_i(m/W) e^{-j2\pi f_c \Delta\tau_i(m/W)} \text{sinc}(\ell - \bar{\tau}W - \Delta\tau_i(m/W)W)$$

Often in practice $f_c\bar{\tau} \sim f_c r/c >> 1$ [1] so it is a reasonable assumption to model $e^{-j2\pi f_c \bar{\tau}} = e^{-j\theta}$ where $\theta \sim Uniform[0, 2\pi]$ and θ is independent of everything else. Note that $\bar{\tau}$ does not depend on m so a particular realization of θ is the same for all components of $\mathbf{h}$. Since $e^{-j\theta}$ has uniformly distributed phase, its distribution does not change if we introduce an arbitrary phase shift ϕ. So $e^{j\phi}e^{-j\theta} \sim e^{-j\theta}$.

It follows that

$$\begin{aligned}
e^{j\phi}\mathbf{h} &= e^{j\phi}e^{-j\theta} \begin{bmatrix} \sum_{i=1}^{N} a_i(m/W) e^{-j2\pi f_c \Delta\tau_i(m/W)} \text{sinc}(\ell - \bar{\tau}W - \Delta\tau_i(m/W)W) \\ \sum_{i=1}^{N} a_i((m+1)/W) e^{-j2\pi f_c \Delta\tau_i((m+1)/W)} \text{sinc}(\ell - \bar{\tau}W - \Delta\tau_i((m+1)/W)W) \\ \vdots \\ \sum_{i=1}^{N} a_i((m+n)/W) e^{-j2\pi f_c \Delta\tau_i((m+n)/W)} \text{sinc}(\ell - \bar{\tau}W - \Delta\tau_i((m+n)/W)W) \end{bmatrix} \\
&=_d e^{-j\theta} \begin{bmatrix} \sum_{i=1}^{N} a_i(m/W) e^{-j2\pi f_c \Delta\tau_i(m/W)} \text{sinc}(\ell - \bar{\tau}W - \Delta\tau_i(m/W)W) \\ \sum_{i=1}^{N} a_i((m+1)/W) e^{-j2\pi f_c \Delta\tau_i((m+1)/W)} \text{sinc}(\ell - \bar{\tau}W - \Delta\tau_i((m+1)/W)W) \\ \vdots \\ \sum_{i=1}^{N} a_i((m+n)/W) e^{-j2\pi f_c \Delta\tau_i((m+n)/W)} \text{sinc}(\ell - \bar{\tau}W - \Delta\tau_i((m+n)/W)W) \end{bmatrix} \\
&=_d \mathbf{h}
\end{aligned}$$

Since this is true for all ϕ, under the previous assumptions $\mathbf{h}$ is circularly symmetric.

EXERCISE 2.17.

1. $h(\tau, t)$ is the response of the channel to an impulse that occurs at time $t - \tau$, i.e., $\delta(t - (t - \tau))$. Replacing $x(t)$ by $\delta(t - (t - \tau))$ in the given expression we obtain:

$$h(\tau, t) = \frac{a}{\sqrt{K}} \sum_{i=0}^{K-1} \delta(\tau - \tau_{\theta_i}(t)).$$

The projection of the velocity vector $\mathbf{v}$ onto the direction of the path at angle θ has a magnitude:

$$v_\theta = |\mathbf{v}| \cos\theta.$$

[1] r is the distance between transmit and receive antennas